

---

# EvoESAP: Non-Uniform Expert Pruning for Sparse MoE

---

Zongfang Liu<sup>1,2\*</sup> Shengkun Tang<sup>3\*</sup> Boyang Sun<sup>3</sup> Zhiqiang Shen<sup>3</sup> Xin Yuan<sup>2</sup>

## Abstract

Sparse Mixture-of-Experts (SMoE) language models achieve strong capability at low per-token compute, yet deployment remains memory- and throughput-bound because the full expert pool must be stored and served. Post-training expert pruning reduces this cost, but most methods focus on which experts to prune within each layer and default to a uniform layer-wise sparsity allocation, even though the allocation can strongly affect performance. We decouple pruning into within-layer expert ranking and across-layer budget allocation, and introduce **Expected Speculative Acceptance Proxy (ESAP)**, a speculative-decoding-inspired, teacher-forced metric that measures how well a pruned model matches the full model. ESAP is bounded and stable, enabling cheap comparison of many candidates without costly autoregressive decoding. Building on ESAP, we propose EvoESAP, an evolutionary searching framework that optimizes a non-uniform layer-wise sparsity allocation under a fixed global budget while holding the within-layer pruning order fixed, making it a plug-and-play method with criteria such as Frequency, EAN, SEER, and REAP. Across 7B–30B SMoE LLMs at 25% and 50% sparsity, EvoESAP consistently discovers non-uniform allocations that improve open-ended generation (up to **+19.6%** on MATH-500 at 50% sparsity) while preserving competitive multiple-choice accuracy compared with uniform pruning at the same sparsity. Code is available in our [GitHub repository](#).

## 1. Introduction

In Transformer (Vaswani et al., 2017) architectures, Sparse Mixture-of-Experts (SMoE) (Shazeer et al., 2017) models

<sup>\*</sup>Equal contribution <sup>1</sup>Zhejiang University, Hangzhou, Zhejiang, China <sup>2</sup>Westlake University, Hangzhou, Zhejiang, China <sup>3</sup>Mohamed bin Zayed University of Artificial Intelligence, Abu Dhabi, United Arab Emirates. Correspondence to: Zhiqiang Shen <zhiqiang.shen@mbzuai.ac.ae>, Xin Yuan <xyuan@westlake.edu.cn>.

replace the dense feed-forward block with multiple expert FFNs and a learned router that dispatches each token to only its top- $k$  experts. The conditional computation mechanism of MoE models enables overall parameters scaling up while retains low computation cost for each token. Modern SMoE LLMs (Jiang et al., 2024; Muennighoff et al., 2024; Liu et al., 2024a; Yang et al., 2025; Meta, 2025; Zeng et al., 2025; Baidu, 2025; Team et al., 2025) deliver strong performance at lower per-token compute, but deployment remains costly because the full expert pool must be stored, stressing memory footprint and serving throughput. Routing analyses from (Huang et al., 2024) further reveal expert-level redundancy and imbalanced expert usage at inference, suggesting room for expert-level compression (Li et al., 2023; Lu et al., 2024b; Zhang et al., 2025; Lee et al., 2025).

Expert-level SMoE compression mainly follows two paradigms: expert merging and expert pruning. Under this lens, recent evidence shows an important caveat for merging: despite strong multiple-choice question (MCQ) answering results, it can degrade open-ended generation quality, plausibly due to irreducible approximation errors introduced by the merge (Lasby et al., 2025). Therefore, we focus on expert pruning in this work. Most prior studies evaluate compression primarily on MCQ answering, while open-ended generation is less explored. Moreover, expert pruning couples two decisions: within-layer expert selection and across-layer allocation of the pruning budget. Most prior work emphasizes selection and defaults to uniform layer-wise ratios. Yet, a consistent lesson from vision pruning (Lee et al., 2020; Liu et al., 2022) and dense LLM pruning (Yin et al., 2023; Lu et al., 2024a; Tang et al., 2025) is that non-uniform layer-wise allocation can be crucial. For SMoEs, existing evidence remains mixed (Muzio et al., 2024; Yang et al., 2024).

In this work, we aim to find the pruned model whose generation ability can match the original model. The natural choice is to apply speculative decoding for the pruned candidate models and the original model and pick the model with the highest acceptance rate relative to the original model. However, this procedure is computation-expensive, especially when the number of the pruned candidates is large, as shown in Table 4. We therefore introduce Expected Speculative Acceptance Proxy (ESAP), a speculative-decoding-inspired, teacher-forced metric that measures how well a

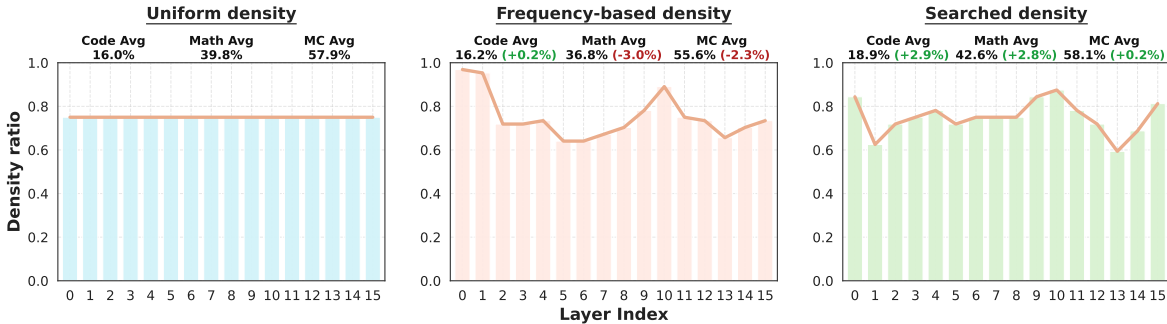


Figure 1. Layer-wise density schedules and performance for OLMoE-1B-7B-0125-Instruct at 25% global sparsity (density = 1 – sparsity). Each panel shows the per-layer remaining expert density under a fixed global pruning budget, using REAP to rank experts in each layer (computed from 1,024 calibration samples from `evol-codealpaca-v1`). **Uniform** prunes the same fraction of experts in every layer. **Frequency-based** ranks experts globally by routing frequency, counts how many experts from each layer fall in the tail 25%, and uses those counts to set layer-wise sparsity. **Searched** finds non-uniform sparsity schedule with EvoESAP under the same budget. Numbers above panels report average performance on Code/Math/MC benchmarks, with deltas relative to uniform. The results imply that given the same pruning metric, non-uniform allocation has the potential to better preserve the model’s capabilities for SMoE expert pruning; however, finding an effective non-uniform allocation is non-trivial, and a poor allocation can harm overall performance.

pruned model matches the full model. ESAP avoids costly autoregressive decoding and instead relies on teacher-forced likelihood evaluations, yielding a bounded, stable, and computationally efficient metric for comparing candidates. Furthermore, we show that, even under the same pruning metric and global sparsity budget, the allocation schedule can be decisive: well-designed non-uniform schedules improve performance, whereas seemingly reasonable heuristics can degrade it, as shown in Figure 1. To find better pruning candidate, we propose **EvoESAP**, an evolutionary search framework that searches for improved non-uniform layer-wise sparsity allocations under a fixed global budget. We decouple pruning into within-layer selection and across-layer budget allocation: given any expert-importance criterion, we first compute a per-layer pruning order, then apply evolutionary optimization to search over allocations, using ESAP as the fitness function for selection. As a plug-and-play method, EvoESAP can be adopted upon any other heuristic pruning metrics such as Frequency, SEER (Muzio et al., 2024), EAN (Jaiswal et al., 2025) and REAP (Lasby et al., 2025). Empirically, we evaluate EvoESAP on OLMoE-1B-7B-0125-Instruct (Muennighoff et al., 2024), ERNIE-4.5-21B-A3B-PT (Baidu, 2025), and Qwen3-30B-A3B-Instruct-2507 (Yang et al., 2025) at 25% and 50% global sparsity. Across four pruning metrics, EvoESAP consistently finds allocations that improve capability over uniform pruning under the same sparsity budget on generative benchmarks. Notably, at 50% global sparsity on ERNIE-4.5-21B-A3B-PT, searching the allocation yields a **+19.6%** gain on MATH-500 (vs. uniform under the same pruning order).

Our contributions can be summarized as:

- We introduce ESAP, a speculative-decoding-inspired, teacher-forced proxy fitness function that enables efficient evaluation of pruning candidates for generation-preserving compression.

- We identify layer-wise budget allocation as a coupled yet under-studied decision in SMoE expert pruning: non-uniform schedules can help, whereas naive ones can hurt. Based on this finding, we propose EvoESAP, an evolutionary search framework for finding improved non-uniform sparsity distributions under a fixed global budget while holding within-layer pruning orders fixed.
- Empirically, across three large SMoE models at 25% and 50% sparsity and four pruning metrics, EvoESAP consistently improves over uniform allocation under the same global budget, with the largest gains on open-ended generation (up to +19.6% on MATH-500 for ERNIE-4.5-21B-A3B-PT at 50% global sparsity).

## 2. Related Work

### 2.1. Expert Pruning

Early work on SMoE pruning is often task- or domain-specific, producing smaller specialized models by removing experts that are rarely useful in a target setting (Chen et al., 2022; Koishkenov et al., 2023). More recent studies instead consider task-agnostic post-training pruning for MoE LLMs. NAAE (Lu et al., 2024b) highlight substantial expert imbalance and propose expert dropping/skipping policies guided by router or expert signals. EEP (Liu et al., 2024b) show that gradient-free evolutionary search can directly optimize which experts to remove under a uniform per-layer pruning ratio. STUN (Lee et al., 2025) proposes a structured-then-unstructured MoE pruning pipeline that clusters experts to prune redundant ones (with selective reconstruction of the remaining expert/router) and then applies unstructured pruning (Sun et al., 2023; Yin et al., 2023) within the surviving experts. Complementary to expert removal, MoE-Pruner (Xie et al., 2024) prune unstructured weights within experts using router hints, reducing compute without changing the number of experts. Most SMoE pruning works are evaluated

mainly on multiple-choice benchmarks, while open-ended generation is largely neglected. REAP (Lasby et al., 2025) argue that pruning better preserves open-ended generation than merging, and their router-weighted expert activation score outperforms frequency-based pruning and the Expert Activation Norm (EAN); notably, EAN is the best among 16 criteria evaluated in (Jaiswal et al., 2025). However, most existing methods implicitly assume uniform sparsity across layers. To the best of our knowledge, explicit discussion of non-uniform sparsity allocation for SMoE pruning remains limited: SEER-MoE (Muzio et al., 2024) empirically suggests that, when allocating sparsity using frequency-based scores, global allocation can outperform layer-wise allocation on MMLU (Hendrycks et al., 2020) for Mixtral-8×7B (Jiang et al., 2024). Whether and how non-uniform sparsity allocation benefits SMoE pruning—especially for open-ended generation—remains an open question.

## 2.2. Expert Merging

Early work on expert merging is exemplified by MEO (He et al., 2023), which dynamically merges the activated experts into a single expert at inference time, using router (gating) scores as the weights. In contrast, more recent merging methods are typically static and rely on clustering to identify redundant experts to consolidate. MC-SMoE (Li et al., 2023) leverages routing statistics to decide which experts to merge: it first performs neuron permutation alignment, then identifies globally dominant experts and assigns the remaining experts as “group members” based on routing behavior, and finally merges each group via activation-frequency-weighted averaging. HC-SMoE (Chen et al., 2024) clusters experts by their output similarity on a calibration set and applies hierarchical clustering to form robust groups; experts within each cluster are then merged using frequency-weighted averaging. DERN (Zhou et al., 2025) extends the granularity from the expert level to the segment level: it first drops redundant experts based on router statistics, then decomposes the dropped experts into neuron-level segments and reassigns these segments to compatible retained experts for merging. As reported in (Lasby et al., 2025), while the state-of-the-art merging method HC-SMoE generally outperforms fine-tuning-free expert pruning methods on MC benchmarks, it can suffer a substantial performance drop on open-ended generation tasks.

## 2.3. Other Compression Methods

Beyond pruning and merging, SMoE models can also be compressed via quantization (Huang et al., 2024) and low-rank decomposition (Gu et al., 2025; He et al., 2025; Li et al.). A growing line of work further combines multiple techniques (He et al., 2024; Liu et al., 2024c). For example, MoE-I<sup>2</sup> (Yang et al., 2024) integrates expert pruning and low-rank decomposition, followed by LoRA fine-

tuning (Hu et al., 2022) to recover performance. In its pruning stage, MoE-I<sup>2</sup> estimates layer importance using a leave-one-out loss increase from removing each expert, allocates per-layer pruning budgets accordingly, and then applies a genetic search to select the experts to retain per layer. Under this criterion, it reports nearly uniform layer-wise sparsity for Mixtral-8×7B (Jiang et al., 2024) and Qwen1.5-MoE-A2.7B (Team, 2024), but a highly non-uniform pattern for DeepSeek-V2-Lite (DeepSeek-AI, 2024), contrasting with SEER-MoE where non-uniform allocation benefits Mixtral-8×7B. Taken together, prior findings paint an inconsistent picture of whether layer-wise sparsity should be uniform or non-uniform across SMoE, leaving the question unclear.

## 3. Method

### 3.1. Sparse Mixture-of-Experts (SMoE) Architecture

Sparse Mixture-of-Experts (SMoE) layers introduce conditional computation by replacing a dense feed-forward network (FFN) with a set of  $n$  expert FFNs  $\{E_i\}_{i=1}^n$  and a router (gating) network that selects only a few experts per token (Shazeer et al., 2017). Given a token hidden state  $h \in \mathbb{R}^d$ , the router produces logits  $z = \mathbf{W}_g h \in \mathbb{R}^n$ , where  $\mathbf{W}_g$  is the router projection. Let  $\mathcal{A}(h) = \text{TopK}(z, k)$  denote the indices of the  $k$  largest logits ( $k \ll n$ ). The sparse gating weights are

$$g_i(h) = \begin{cases} \frac{\exp(z_i)}{\sum_{j \in \mathcal{A}(h)} \exp(z_j)}, & i \in \mathcal{A}(h), \\ 0, & i \notin \mathcal{A}(h), \end{cases} \quad (1)$$

and the MoE output is the weighted mixture of the selected experts:

$$y(h) = \sum_{i \in \mathcal{A}(h)} g_i(h) E_i(h). \quad (2)$$

Because  $g(h)$  has only  $k$  nonzero entries, only the selected experts are evaluated, so the per-token compute is approximately proportional to  $k$  while total capacity scales with the number of experts (Fedus et al., 2022).

### 3.2. Problem Formulation

The goal of expert pruning is to obtain a compressed SMoE model that preserves the full model’s behavior while reducing deployment cost (e.g., memory usage). This entails two coupled choices: which experts to remove (within-layer selection) and how many to remove per layer (across-layer allocation). Most prior work focuses on selection while implicitly adopting uniform per-layer pruning, thereby overlooking the allocation axis. We therefore decouple pruning into two steps: we first fix a per-layer pruning order (e.g., from REAP), and then use an evolutionary search to optimize a non-uniform layer-wise allocation under the same

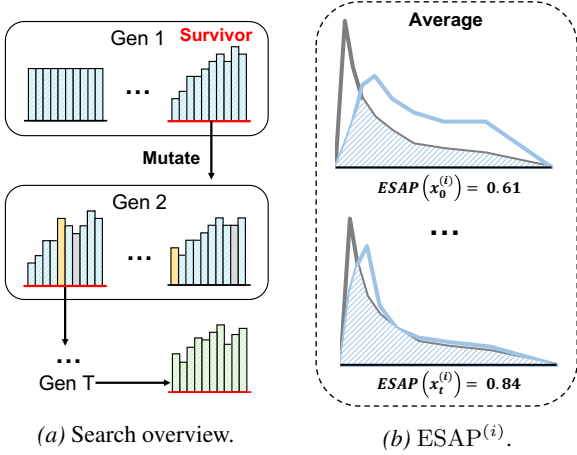


Figure 2. **Overview of EvoESAP.** (a) **Evolutionary search with budget-preserving level-switch mutation.** Histograms visualize the layer-wise density distribution of each candidate model (density =  $1 - \text{sparsity}$ ) induced by an allocation  $\mathbf{r}$  (experts removed per layer) under a fixed global budget  $B$ . Offspring are generated from the top  $m$  survivors by a *level-switch* that transfers  $\Delta$  units of pruning budget between two layers (gray: decrease; yellow: increase), keeping  $\sum_{\ell} r_{\ell} = B$  unchanged. (b) **ESAP as per-sample fitness.** Under teacher forcing, ESAP scores a sample by the full-vocabulary overlap between the baseline/target next-token distribution (dark gray,  $p(\cdot | x)$ ) and the candidate/draft distribution (blue,  $q(\cdot | x)$ ), averaged over answer-token positions (higher is better; see Equation (12)).

global budget, guided by ESAP (Section 3.4), a speculative-decoding-inspired, behavior-preserving fitness function.

**Per-layer pruning order.** Consider an SMoE model with  $L$  MoE layers. Layer  $\ell \in \{1, \dots, L\}$  contains  $n_{\ell}$  experts  $\{E_{\ell,1}, \dots, E_{\ell,n_{\ell}}\}$  (typically  $n_{\ell} \equiv n$  in practice). We compute an importance score  $s_{\ell,j}$  for each expert  $E_{\ell,j}$  using a chosen criterion (e.g., REAP), and define a layer-wise pruning order by sorting experts in ascending importance:  $\pi_{\ell} = \text{argsort}_{j \in \{1, \dots, n_{\ell}\}}(s_{\ell,j})$  where  $\pi_{\ell}$  is a permutation of  $\{1, \dots, n_{\ell}\}$  such that  $s_{\ell,\pi_{\ell}(1)} \leq \dots \leq s_{\ell,\pi_{\ell}(n_{\ell})}$ . Given a layer-wise pruning budget  $r_{\ell} \in \{0, 1, \dots, n_{\ell} - k_{\ell}\}$  (to ensure at least  $k_{\ell}$  experts remain for top- $k_{\ell}$  routing), we prune the  $r_{\ell}$  least important experts:  $\mathcal{P}_{\ell}(r_{\ell}) = \{\pi_{\ell}(j)\}_{j=1}^{r_{\ell}}$ .

### 3.3. Evolutionary Search with Level-Switch Mutation

**Search space, constraint, and objective.** With the per-layer pruning orders  $\{\pi_{\ell}\}$  fixed, the remaining degree of freedom is the layer-wise sparsity allocation under a fixed global pruning budget. We therefore search over integer allocation vectors  $\mathbf{r} = (r_1, \dots, r_L)$ , where  $r_{\ell}$  is the number of experts removed in layer  $\ell$  and  $B$  is the *global* pruning budget (total number of experts removed across all MoE layers). Concretely, we solve

$$\begin{aligned} \mathbf{r}^* \in \arg \max_{\mathbf{r} \in \mathbb{Z}^L} f(\mathbf{r}; \mathcal{D}_{\text{search}}) \\ \text{s.t. } \sum_{\ell=1}^L r_{\ell} = B, \quad 0 \leq r_{\ell} \leq n_{\ell} - k_{\ell}, \forall \ell. \end{aligned} \quad (3)$$

so that at least  $k_{\ell}$  experts remain in every layer for top- $k_{\ell}$  routing. The search set  $\mathcal{D}_{\text{search}}$  is used only for ESAP fitness evaluation; the pruning orders  $\{\pi_{\ell}\}$  are computed once from the chosen importance criterion on its own calibration data.

**Initialization.** We initialize population  $\mathcal{S}^{(0)}$  of size  $P$  with a mixture of structured patterns and random feasible allocations: (i) a uniform allocation, (ii) several patterned allocations that concentrate pruning in different layer regions (e.g., early-heavy, middle-heavy, late-heavy), and (iii) the remaining individuals sampled uniformly from all feasible allocations that satisfy the global budget.

**Selection.** We evaluate each candidate  $\mathbf{r} \in \mathcal{S}^{(t)}$  and keep the top  $m$  survivors:

$$\mathcal{S}_{\text{elite}}^{(t)} = \text{TopM}(\{\mathbf{r} \in \mathcal{S}^{(t)}\}; f(\mathbf{r}), m), \quad (4)$$

where  $\text{TopM}$  returns the  $m$  highest-fitness candidates. We carry  $\mathcal{S}_{\text{elite}}^{(t)}$  into the next generation and generate  $P - m$  offspring via mutation.

**Level-switch mutation.** To generate an offspring, we sample a parent  $\mathbf{r}$  from  $\mathcal{S}_{\text{elite}}^{(t)}$  and apply a budget-preserving *level-switch* operator that transfers pruning budget between two layers while keeping the global constraint unchanged. A single level-switch step samples two distinct layers  $a \neq b$  and a transfer size  $\Delta \in \{1, \dots, \Delta_{\text{max}}\}$ , and updates

$$r'_{\ell} = \begin{cases} r_{\ell} + \Delta, & \ell = a, \\ r_{\ell} - \Delta, & \ell = b, \\ r_{\ell}, & \text{otherwise,} \end{cases} \quad (5)$$

subject to feasibility  $0 \leq r_b - \Delta$  and  $r_a + \Delta \leq n_a - k_a$ . If the sampled  $(a, b, \Delta)$  is infeasible, we resample until Equation (5) yields a valid allocation.

We apply this operator multiple times per offspring by composing  $\tau$  feasible level-switch steps, where the mutation count is

$$\tau = \min(U\{1, \dots, \tau_{\text{max}}\}, U\{1, \dots, \tau_{\text{max}}\}), \quad (6)$$

and  $U\{1, \dots, \tau_{\text{max}}\}$  denotes a discrete uniform draw from  $\{1, \dots, \tau_{\text{max}}\}$  (two draws are independent). This choice biases mutations toward small local reallocations (exploitation), while still occasionally producing larger jumps through multiple composed transfers (exploration).

**Termination and output.** We run the search for  $T$  generations and output the best-found allocation

$$\mathbf{r}^* = \arg \max_{\mathbf{r} \in \cup_{t=0}^T \mathcal{S}^{(t)}} f(\mathbf{r}; \mathcal{D}_{\text{search}}), \quad (7)$$

and instantiate the pruned model by applying  $\{\mathcal{P}_{\ell}(r_{\ell}^*)\}_{\ell=1}^L$  from Section 3.2. Pseudocode of evolutionary searching is provided in Appendix A.

### 3.4. Expected Speculative Acceptance Proxy (ESAP)

In our evolutionary search, we seek non-uniform layer-wise sparsity allocation that keep the pruned candidate closer to the baseline (full model). Accordingly, our fitness should (i) correlate with behavioral similarity to the baseline and (ii) be cheap enough to evaluate for hundreds/thousands of candidates.

**Speculative decoding as a compatibility signal.** Speculative decoding (Leviathan et al., 2023; Chen et al., 2023) accelerates inference by letting a lightweight draft model propose tokens, while the baseline/target model verifies and either accepts them or falls back to its own token. The similar the output the two models are, the faster the inference. Intuitively, if a candidate can serve as an effective draft model for its full version then it’s behavior should be close to full model, suggesting the speculative acceptance rate as a natural compatibility signal. Let  $p(\cdot | x)$  denote the baseline/target next-token distribution given context (prefix)  $x$ , and let  $q(\cdot | x)$  denote the candidate/draft distribution. When the draft proposes a token  $y \sim q(\cdot | x)$  from draft, the standard acceptance probability is

$$\alpha(x, y) = \min\left(1, \frac{p(y | x)}{q(y | x)}\right), \quad (8)$$

together with the standard rejection correction step guarantees that the overall decoded token distribution exactly matches the target model (Leviathan et al., 2023). However, directly estimating speculative acceptance inside an inner-loop search is expensive: it requires autoregressive generation for many prompts, running *both* models, and the measured acceptance depends on the sampled trajectory, block size, and prefix drift after rejections. As shown in Table 4, this is prohibitively expensive and introduces substantial variance, making it unsuitable for ranking hundreds or thousands of candidates.

**SAP: a dataset-level single-token acceptance proxy.** A natural way to remove trajectory dependence while staying close to the speculative-decoding acceptance test is to evaluate Equation (8) on fixed, teacher-forced contexts from a search (calibration) dataset. Let  $\mathcal{D}_{\text{search}} = \{(u^{(i)}, a^{(i)})\}_{i=1}^N$  contain  $N$  prompt–answer pairs. For each sample  $i$ , we teacher-force on  $(u^{(i)}, a^{(i)})$  but score only answer-token positions:  $\mathcal{I}^{(i)}$  indexes the next-token contexts whose *next token* lies in  $a^{(i)}$ . For each  $t \in \mathcal{I}^{(i)}$ , let  $x_t^{(i)}$  be the corresponding prefix context, and let  $p(\cdot | x_t^{(i)})$  and  $q(\cdot | x_t^{(i)})$  denote the baseline and candidate next-token distributions.

At a single context  $x_t^{(i)}$ , the *Speculative Acceptance Proxy* (SAP) draws one proposal  $\hat{y}_t^{(i)} \sim q(\cdot | x_t^{(i)})$  and evaluates its speculative acceptance probability:

$$\text{SAP}(x_t^{(i)}) \triangleq \min\left(1, \frac{p(\hat{y}_t^{(i)} | x_t^{(i)})}{q(\hat{y}_t^{(i)} | x_t^{(i)})}\right). \quad (9)$$

We average over answer positions within each sample,

$$\text{SAP}^{(i)} \triangleq \frac{1}{|\mathcal{I}^{(i)}|} \sum_{t \in \mathcal{I}^{(i)}} \text{SAP}(x_t^{(i)}), \quad (10)$$

and then report the dataset-level score as the mean over samples:

$$\text{SAP} \triangleq \frac{1}{N} \sum_{i=1}^N \text{SAP}^{(i)}. \quad (11)$$

Because SAP is evaluated on shared, fixed teacher-forced contexts (answer tokens only), it avoids prefix drift and less computation time. However, it remains a Monte-Carlo estimator since it depends on the sampled proposal  $\hat{y}_t^{(i)}$ , which can introduce variance.

**ESAP: an expected acceptance proxy of speculative decoding.** SAP in Equation (9) depends on a sampled proposal  $\hat{y}_t^{(i)} \sim q(\cdot | x_t^{(i)})$ , which can introduce variance. We remove this Monte-Carlo noise by taking the expectation of the same acceptance test under the draft distribution. For each teacher-forced context  $x_t^{(i)}$ , we define

$$\text{ESAP}(x_t^{(i)}) \triangleq \mathbb{E}_{y \sim q(\cdot | x_t^{(i)})} \left[ \min\left(1, \frac{p(y | x_t^{(i)})}{q(y | x_t^{(i)})}\right) \right]. \quad (12)$$

Expanding the expectation yields a closed form:

$$\text{ESAP}(x_t^{(i)}) = \sum_{v \in \mathcal{V}} q(v | x_t^{(i)}) \min\left(1, \frac{p(v | x_t^{(i)})}{q(v | x_t^{(i)})}\right) \quad (13)$$

$$= \sum_{v \in \mathcal{V}} \min(p(v | x_t^{(i)}), q(v | x_t^{(i)})), \quad (14)$$

using  $q(v) \min(1, p(v)/q(v)) = \min(p(v), q(v))$  for each vocabulary token  $v$ . Analogous to Equation (11), we average ESAP over answer positions within each sample:

$$\text{ESAP}^{(i)} \triangleq \frac{1}{|\mathcal{I}^{(i)}|} \sum_{t \in \mathcal{I}^{(i)}} \text{ESAP}(x_t^{(i)}), \quad (15)$$

and report the dataset-level score as

$$\text{ESAP} \triangleq \frac{1}{N} \sum_{i=1}^N \text{ESAP}^{(i)}. \quad (16)$$

Figure 2(b) visualizes  $\text{ESAP}^{(i)}$  as the token-level overlap between  $p(\cdot | x_t^{(i)})$  and  $q(\cdot | x_t^{(i)})$  averaged over answer positions. Moreover, since  $\text{ESAP}(x) = \sum_{v \in \mathcal{V}} \min(p(v | x), q(v | x))$ , it also can be viewed as the complement of total variation:

$$\text{ESAP}(x) = 1 - \text{TV}(p(\cdot | x), q(\cdot | x)), \quad (17)$$

where  $\text{TV}(p, q) := \frac{1}{2} \sum_{v \in \mathcal{V}} |p(v) - q(v)|$  (derivation in Appendix B).

Table 1. MC and open-ended generation benchmark results for OLMoE and ERNIE. Under the same within-layer pruning order and global sparsity, EvoESAP’s searched non-uniform allocation generally improves open-ended generation compared with uniform pruning.

Model	Sparsity	Method	Eval+	Coding		WildBench	Math			MC MC Avg		
				LiveCode	Avg		GSM8K	MATH-500	Avg			
OLMoE	Full		0.341	0.033	0.187	0.444	0.682	0.222	0.452	0.653		
		EAN	UNI ESAP	<b>0.343</b> 0.312	0.022 <b>0.027</b>	<b>0.183</b> 0.170	<b>0.269</b> 0.258	<b>0.585</b> 0.576	0.190 <b>0.232</b>	0.387 <b>0.404</b>	<b>0.551</b> 0.543	
	25%	SEER	UNI ESAP	<b>0.339</b> 0.306	<b>0.027</b> 0.022	<b>0.183</b> 0.164	0.253 <b>0.254</b>	0.577 <b>0.601</b>	0.204 <b>0.248</b>	0.390 <b>0.424</b>	<b>0.545</b> 0.539	
		Freq	UNI ESAP	0.341 <b>0.342</b>	0.022 0.022	0.182 0.182	<b>0.265</b> 0.244	0.591 <b>0.596</b>	<b>0.220</b> 0.208	<b>0.405</b> <b>0.402</b>	<b>0.547</b> 0.539	
		REAP	UNI ESAP	0.314 <b>0.344</b>	0.005 <b>0.033</b>	0.160 <b>0.189</b>	<b>0.292</b> 0.279	0.596 <b>0.636</b>	0.200 <b>0.216</b>	0.398 <b>0.426</b>	0.579 <b>0.581</b>	
		Full		0.867	0.247	0.557	0.479	0.829	0.780	0.804	0.721	
	ERNIE	25%	EAN	UNI ESAP	0.827 <b>0.832</b>	0.214 <b>0.225</b>	0.520 <b>0.528</b>	<b>0.377</b> 0.333	0.815 <b>0.823</b>	0.748 <b>0.772</b>	0.781 <b>0.797</b>	0.669 <b>0.675</b>
			SEER	UNI ESAP	0.830 <b>0.838</b>	<b>0.214</b> 0.203	<b>0.522</b> 0.520	<b>0.301</b> 0.291	<b>0.804</b> <b>0.804</b>	<b>0.736</b> 0.728	<b>0.770</b> 0.766	0.634 <b>0.638</b>
		Freq	UNI ESAP	<b>0.818</b> 0.811	0.181 <b>0.236</b>	0.499 <b>0.524</b>	0.314 <b>0.316</b>	0.810 <b>0.815</b>	0.692 <b>0.716</b>	0.751 <b>0.765</b>	0.636 <b>0.647</b>	
			REAP	UNI ESAP	0.823 <b>0.833</b>	<b>0.231</b> 0.209	<b>0.527</b> 0.521	0.354 <b>0.376</b>	<b>0.821</b> 0.814	0.730 <b>0.752</b>	0.775 <b>0.783</b>	0.667 <b>0.672</b>
50%		EAN	UNI ESAP	0.636 <b>0.659</b>	<b>0.148</b> 0.143	0.392 <b>0.401</b>	0.156 <b>0.186</b>	<b>0.748</b> 0.744	0.542 <b>0.558</b>	0.645 <b>0.651</b>	<b>0.585</b> 0.582	
		SEER	UNI ESAP	0.698 <b>0.709</b>	0.170 <b>0.181</b>	0.434 <b>0.445</b>	0.130 <b>0.151</b>	0.555 <b>0.640</b>	0.418 <b>0.508</b>	0.487 <b>0.574</b>	<b>0.551</b> 0.547	
		Freq	UNI ESAP	0.647 0.647	<b>0.143</b> 0.126	<b>0.395</b> 0.387	0.130 <b>0.151</b>	0.522 <b>0.631</b>	0.272 <b>0.468</b>	0.397 <b>0.549</b>	<b>0.565</b> 0.557	
			REAP	UNI ESAP	0.730 <b>0.737</b>	<b>0.192</b> 0.187	0.461 <b>0.462</b>	<b>0.215</b> 0.205	0.695 <b>0.718</b>	<b>0.598</b> 0.578	0.646 <b>0.648</b>	0.575 0.575

## 4. Experiment

### 4.1. Experimental Setup

**Models and Data.** We validate EvoESAP on SMOE LLMs spanning the 7B–30B scale: OLMoE-1B-7B-0125-Instruct (Muennighoff et al., 2024), ERNIE-4.5-21B-A3B-PT (Baidu, 2025), and Qwen3-30B-A3B-Instruct-2507 (Yang et al., 2025). We instantiate within-layer pruning orders using four expert-importance criteria: activation Frequency, SEER soft counting (Muzio et al., 2024), Expert Activation Norm (EAN) (Jaiswal et al., 2025), and REAP (Lasby et al., 2025). In Table 1 and Table 2, all pruning metrics are calibrated with 1,024 samples from `evol-codealpaca-v1` and searched with 64 samples from `tulu-3-sft-personas-math`.

**Evaluation.** For evaluation, following (Lasby et al., 2025), our multiple-choice (MC) evaluation suite includes AI2 Reasoning Challenge (ARC-C/ARC-E) (Clark et al., 2018), BoolQ (Clark et al., 2019), HellaSwag (Zellers et al., 2019), MMLU (Hendrycks et al., 2020), OpenBookQA (OBQA) (Mihaylov et al., 2018), Recognizing Textual Entailment (RTE) (Bentivogli et al., 2009), and WinoGrande (WinoG.) (Sakaguchi et al., 2021). We evaluate all MC tasks using the standard log-likelihood protocol implemented in `lm-eval-harness` (Gao et al., 2021). For open-ended generation, we consider code generation on EvalPlus (Liu

et al., 2023) and 182 LiveCodeBench (Jain et al., 2024) problems collected between January and April 2025; math generation on GSM8K (Cobbe et al., 2021) and MATH-500 (Hendrycks et al., 2021) using the `evalscope` framework (Team); and creative writing on 146 prompts sampled from WildBench (Lin et al., 2024), where we use `gpt-oss-120b` (OpenAI, 2025) as the judge to score model responses. All evaluations are in zero-shot setting.

**Implementation Details.** For generation tasks, we use greedy decoding (temperature = 0.0) for fair comparisons. For Qwen3-30B-A3B, we disable reasoning on all tasks by setting `enable_thinking=False` in the chat template. Across all variants, we fix the evolutionary-search hyperparameters to ensure fair comparison: seed 42, population size  $P=32$ , elite size  $m=4$ , maximum transfer  $\Delta_{\max}=4$ , and maximum composed steps  $\tau_{\max}=3$ . We run the search for  $T=50$  generations on OLMoE,  $T=20$  on ERNIE, and  $T=10$  on Qwen3.

### 4.2. Main results

**Performance Comparison** Tables 1 and 2 compare UNI (uniform layer-wise sparsity) against the non-uniform allocation found by EvoESAP (reported as ESAP), while holding the within-layer pruning order fixed for each criterion (EAN, SEER, Frequency, REAP) and keeping the same

Table 2. MC and open-ended generation benchmark results for Qwen3.

Model	Sparsity	Method	Eval+	Coding			WildBench	GSM8K	Math		MC Avg
				LiveCode	Avg				MATH-500	Avg	
Qwen3	Full			0.871	0.368	0.619	0.644	0.923	0.802	0.863	0.737
		EAN	UNI	<b>0.871</b>	0.363	<b>0.617</b>	<b>0.517</b>	<b>0.902</b>	0.748	0.825	0.628
	ESAP		0.858	0.363	0.611	0.439	0.901	<b>0.752</b>	<b>0.827</b>	<b>0.634</b>	
	25%	SEER	UNI	0.851	0.363	0.607	0.449	0.891	0.636	0.764	0.561
			ESAP	<b>0.861</b>	<b>0.385</b>	<b>0.623</b>	<b>0.482</b>	<b>0.897</b>	<b>0.716</b>	<b>0.806</b>	<b>0.577</b>
		Freq	UNI	<b>0.862</b>	0.357	0.609	0.446	0.891	0.658	0.774	0.558
			ESAP	0.860	<b>0.396</b>	<b>0.628</b>	<b>0.463</b>	<b>0.907</b>	<b>0.734</b>	<b>0.821</b>	<b>0.572</b>
	REAP	UNI	<b>0.872</b>	<b>0.385</b>	<b>0.629</b>	<b>0.565</b>	<b>0.910</b>	<b>0.784</b>	<b>0.847</b>	<b>0.706</b>	
		ESAP	0.835	0.324	0.580	0.533	0.886	0.778	0.832	0.665	
	50%	EAN	UNI	<b>0.846</b>	0.341	<b>0.594</b>	0.231	0.833	0.456	0.644	0.516
			ESAP	0.839	<b>0.346</b>	0.593	<b>0.243</b>	<b>0.846</b>	<b>0.494</b>	<b>0.670</b>	<b>0.518</b>
		SEER	UNI	0.700	0.247	0.473	0.112	<b>0.605</b>	0.144	0.374	<b>0.455</b>
			ESAP	<b>0.767</b>	<b>0.264</b>	<b>0.516</b>	<b>0.142</b>	0.550	<b>0.220</b>	<b>0.385</b>	0.446
		Freq	UNI	0.700	0.225	0.462	0.110	0.592	0.128	0.360	0.450
			ESAP	<b>0.781</b>	<b>0.275</b>	<b>0.528</b>	<b>0.182</b>	<b>0.697</b>	<b>0.214</b>	<b>0.455</b>	<b>0.510</b>
		REAP	UNI	0.828	<b>0.341</b>	0.585	<b>0.299</b>	<b>0.872</b>	<b>0.798</b>	<b>0.835</b>	<b>0.596</b>
ESAP			<b>0.855</b>	0.335	<b>0.595</b>	0.267	0.867	0.792	0.830	0.585	

Table 3. Search cost and GPU memory usage. Search Time is the wall-clock time for the full evolutionary search run. Memory reports GPU memory usage of loading the final compressed model alongside the full baseline (pruned/full) with bfloat16.

Model	GPU	Generations	Time (h)	Memory (GB)
OLMoE-7B	1×L40S	50	5.8	9.89 / 12.9
ERNIE-21B	2×L40S	20	5.0	31.17 / 40.66
Qwen3-30B	2×L40S	10	5.2	43.42 / 56.92

Table 4. Comparison of true speculative-decoding acceptance (SPEC-DEC) and the proposed ESAP. ESAP reduces the searching time from 29.49h to 1.64h.

Fitness	GPU	Time (h)	Code Avg	WildBench	MC Avg
SPEC-DEC	2×L40S	29.49	0.171	<b>0.269</b>	<b>0.565</b>
ESAP	1×L40S	<b>1.64</b>	<b>0.173</b>	0.256	0.557

global sparsity budget. Across models, EvoESAP most consistently improves open-ended generation especially on coding and math, while MC typically changes only slightly; moreover, the gains generally grow as sparsity increases. On OLMoE at 25% sparsity, EvoESAP with REAP yields clear generation gains: coding improves by 2.9%, math by 2.8%, while MC remains essentially unchanged (+0.2%). This shows that even under an identical pruning metric, optimizing where capacity is kept can materially strengthen generation-preserving pruning. For ERNIE, improvements are smaller at 25% (e.g., Frequency: Code Avg +2.5%, Math Avg +1.4%, MC +1.1%), but become much larger at 50%, where allocation is more consequential for generation. For example, SEER improves Math Avg by +8.7% with only a small MC change (−0.4%), and Frequency yields an even larger Math Avg gain of +15.2% (MATH-500 +19.6%). On Qwen3, EvoESAP most strongly benefits weaker criteria whose UNI allocations leave clear headroom. At 50% sparsity, Frequency improves Code Avg by 6.6%, WildBench

by 7.2%, Math Avg by 9.5%, and MC by 6.0%. At 25% sparsity, both SEER and Frequency improve broadly. In contrast, when the pruning order already preserves the most important experts across layers (e.g., REAP on Qwen3 at 25%), uniform allocation can be close to a well-balanced schedule and re-allocation offers limited benefit—or can even hurt (−4.9% Code Avg, −4.1% MC). We hypothesize that in such regimes the key experts are already retained across layers, making the marginal value of redistributing the remaining budget smaller. The tables also underscore that the “best” pruning criterion is not universal across models. At 25% sparsity, REAP is strongest on Qwen3 (uniform REAP achieves the best Code Avg and MC), whereas on OLMoE the same uniform REAP is comparatively weak on coding, even trailing the simpler Frequency (−2.2% on Code Avg). This non-universality suggests treating allocation as an orthogonal, reusable improvement axis: regardless of which criterion is strongest for a given model, EvoESAP can further optimize where capacity is retained under the same global budget, providing a stable pathway to improve pruning—especially at higher sparsity where preserving open-ended generation quality becomes increasingly sensitive to allocation. Detailed results on specific sub-benchmarks can be found in [Appendix F](#) and the visualization of the searched non-uniform sparsity distribution can be found in [Appendix E](#). We also report results when using C4 ([Allen Institute for AI, 2024](#)) as the calibration set for computing pruning orders in [Appendix D](#). Overall, EvoESAP continues to deliver consistent improvements over uniform allocation under the same global budget. However, comparing these C4-calibrated results with those in Table 1 shows that expert pruning can be highly sensitive to the choice of calibration data. For example, although C4 calibration slightly improves MC performance for uniform REAP (1.7%), it leads to roughly a 40% drop on code benchmarks.

Table 5. Ablations of fitness choice and search sample size at 25% global sparsity on OLMoE. The results show that our method is robust to fitness choice and sample size, and our ESAP achieves higher performance on coding and math tasks.

Ablation	Value	Coding			Creative Writing WildBench	Math			MC MC Avg
		Eval+	LiveCode	Code Avg		GSM8K	MATH-500	Math Avg	
Fitness	KL	0.331	0.016	0.174	0.285	0.595	0.216	0.405	0.582
	NLL	0.334	0.016	0.175	<b>0.295</b>	0.619	<b>0.230</b>	0.424	0.576
	SAP	0.339	0.005	0.172	0.289	0.622	0.218	0.420	<b>0.584</b>
	ESAP (Ours)	<b>0.344</b>	<b>0.033</b>	<b>0.189</b>	0.279	<b>0.636</b>	0.216	<b>0.426</b>	0.581
Samples	8	0.320	0.022	0.171	0.290	0.627	<b>0.228</b>	0.427	0.576
	16	0.324	0.016	0.170	<b>0.291</b>	0.630	0.226	0.428	0.579
	32	0.339	0.016	0.178	0.285	<b>0.645</b>	0.222	<b>0.433</b>	<b>0.582</b>
	64	<b>0.344</b>	<b>0.033</b>	<b>0.189</b>	0.279	0.636	0.216	0.426	0.581
	128	0.347	0.011	0.179	0.286	0.625	0.214	0.419	0.579

This sensitivity highlights that pruning methods should be evaluated under the same calibration set for fair comparison. Based on our results and the evidence in REAP (Lasby et al., 2025), we recommend `evol-codealpaca-v1` as a calibration dataset for pruning, as it yields a better balance between open-ended generation and MC performance.

**Search time and memory usage after compression.** Table 3 reports the practical cost of running EvoESAP at 25% global sparsity: the required number of GPUs and the wall-clock search time for the full evolutionary run (with the model-specific generation counts shown in the table). We also report the peak GPU memory required to load the *final* compressed model for inference, alongside the full baseline under the same `bfloat16` setting. This inference-time measurement reflects the true memory reduction delivered by pruning, independent of search-time overhead.

### 4.3. Ablation Study

All experiments in this section use OLMoE-1B-7B-0125-Instruct and adopt REAP calibrated on `evol-codealpaca-v1`, as the within-layer pruning order. Unless otherwise specified, we follow the same experimental settings as in Section 4.1.

**Speculative Decoding As Fitness.** To validate ESAP as a proxy for speculative-decoding compatibility, we additionally run evolutionary search using the *true* speculative-decoding acceptance (SPEC-DEC) as the fitness. We summarize the comparison in Table 4, where we run the search on `evol-codealpaca-v1` for 30 generations. While directly optimizing SPEC-DEC yields only marginal gains, it is impractical as an inner-loop fitness: it requires running both the draft and verifier with large KV caches and performing autoregressive decoding, substantially increasing GPU demand and wall-clock evaluation cost. In contrast, ESAP achieves comparable performance while using fewer GPUs and reducing search time by  $\sim 18\times$ , supporting ESAP as an effective proxy for speculative-decoding compatibility.

**Comparison with other teacher-forcing fitness functions.** To examine the effectiveness of our proposed ESAP, we compare it against three alternative fitness signals: Kullback-

Leibler divergence (KL), negative log-likelihood (NLL), and speculative acceptance proxy (SAP). Results are reported in Table 5. ESAP provides the strongest and most consistent generation-preserving compression: it attains the best *coding* performance across Eval+, LiveCode, and Code Avg, and also achieves the highest *overall math* score with the strongest GSM8K. Importantly, ESAP remains competitive on multiple-choice evaluation, coming close to the best MC score. This suggests that ESAP is an effective fitness function for generation-preserving sparsity allocation.

**Sensitivity to the number of search data.** Table 5 also examines the effect of search sample size. Overall, once we use a modest number of samples, search quality is largely stable and does not improve monotonically with more data. In particular, 32–64 samples already capture the benefit of EvoESAP: 64 samples delivers the strongest coding results, while 32 samples achieves the best Math Avg and MC Avg, and also attains the highest GSM8K score. With only 8–16 samples, performance remains competitive but is slightly weaker, consistent with a noisier fitness estimate. By contrast, increasing to 128 samples provides no additional gains and can even slightly degrade performance. We therefore adopt 64 samples as our default setting in our experiments.

## 5. Conclusion

We introduced EvoESAP, a framework for SMoE expert pruning that finds the non-uniform layer-wise sparsity allocation which is mostly omitted by previous works. Given any within-layer pruning order (e.g., Frequency, SEER, EAN, or REAP), EvoESAP searches over integer layer-wise budgets via a budget-preserving level-switch mutation, guided by Expected Speculative Acceptance Proxy (ESAP), a speculative-decoding-inspired, teacher-forced overlap score between the baseline and pruned next-token distributions. Across 7B–30B SMoE models and 25%–50% sparsity, the non-uniform schedules discovered by EVOESAP consistently improve capability over uniform pruning under the same pruning metric and global budget, with the most reliable gains on open-ended generation and larger benefits at higher sparsity.

## Impact Statement

This paper proposes finetuning-free pruning for SMOE language models that reduces deployment cost (e.g., GPU memory usage) while aiming to preserve open-ended generation quality. The main positive impact is improved efficiency, which can lower energy and financial costs and broaden access to capable models in resource-constrained settings. However, compression does not mitigate inherent risks of language models (e.g., biased or harmful outputs), and cheaper deployment may increase both beneficial and harmful use; compressed models should therefore be re-evaluated for safety, robustness, and bias and deployed with appropriate safeguards consistent with the original model’s intended use and license.

## References

- Allen Institute for AI. allenai/c4 · datasets at Hugging Face. <https://huggingface.co/datasets/allenai/c4>, August 2024.
- Baidu. Ernie 4.5 technical report. Technical report, Baidu, 2025. URL [https://ernie.baidu.com/blog/publication/ERNIE\\_Technical\\_Report.pdf](https://ernie.baidu.com/blog/publication/ERNIE_Technical_Report.pdf). Technical report.
- Bentivogli, L., Clark, P., Dagan, I., and Giampiccolo, D. The fifth pascal recognizing textual entailment challenge. *TAC*, 7(8):1, 2009.
- Chen, C., Borgeaud, S., Irving, G., Lespiau, J.-B., Sifre, L., and Jumper, J. Accelerating large language model decoding with speculative sampling. *arXiv preprint arXiv:2302.01318*, 2023.
- Chen, I., Liu, H.-S., Sun, W.-F., Chao, C.-H., Hsu, Y.-C., Lee, C.-Y., et al. Retraining-free merging of sparse moe via hierarchical clustering. *arXiv preprint arXiv:2410.08589*, 2024.
- Chen, T., Huang, S., Xie, Y., Jiao, B., Jiang, D., Zhou, H., Li, J., and Wei, F. Task-specific expert pruning for sparse mixture-of-experts. *arXiv preprint arXiv:2206.00277*, 2022.
- Clark, C., Lee, K., Chang, M.-W., Kwiatkowski, T., Collins, M., and Toutanova, K. Boolq: Exploring the surprising difficulty of natural yes/no questions. *arXiv preprint arXiv:1905.10044*, 2019.
- Clark, P., Cowhey, I., Etzioni, O., Khot, T., Sabharwal, A., Schoenick, C., and Tafjord, O. Think you have solved question answering? try arc, the ai2 reasoning challenge. *arXiv preprint arXiv:1803.05457*, 2018.
- Cobbe, K., Kosaraju, V., Bavarian, M., Chen, M., Jun, H., Kaiser, L., Plappert, M., Tworek, J., Hilton, J., Nakano, R., et al. Training verifiers to solve math word problems. *arXiv preprint arXiv:2110.14168*, 2021.
- DeepSeek-AI. Deepseek-v2: A strong, economical, and efficient mixture-of-experts language model, 2024.
- Fedus, W., Zoph, B., and Shazeer, N. Switch transformers: Scaling to trillion parameter models with simple and efficient sparsity. *Journal of Machine Learning Research*, 23(120):1–39, 2022.
- Gao, L., Tow, J., Biderman, S., Black, S., DiPofi, A., Foster, C., Golding, L., Hsu, J., McDonell, K., Muennighoff, N., et al. A framework for few-shot language model evaluation. *Zenodo*, 2021.
- Gu, H., Li, W., Li, L., Zhu, Q., Lee, M., Sun, S., Xue, W., and Guo, Y. Delta decompression for moe-based llms compression. *arXiv preprint arXiv:2502.17298*, 2025.
- He, S., Fan, R.-Z., Ding, L., Shen, L., Zhou, T., and Tao, D. Merging experts into one: Improving computational efficiency of mixture of experts. *arXiv preprint arXiv:2310.09832*, 2023.
- He, S., Dong, D., Ding, L., and Li, A. Towards efficient mixture of experts: A holistic study of compression techniques. *arXiv preprint arXiv:2406.02500*, 2024.
- He, Y., Liu, Y., Liang, C., and Awadalla, H. H. Efficiently editing mixture-of-experts models with compressed experts. *arXiv preprint arXiv:2503.00634*, 2025.
- Hendrycks, D., Burns, C., Basart, S., Zou, A., Mazeika, M., Song, D., and Steinhardt, J. Measuring massive multitask language understanding. *arXiv preprint arXiv:2009.03300*, 2020.
- Hendrycks, D., Burns, C., Kadavath, S., Arora, A., Basart, S., Tang, E., Song, D., and Steinhardt, J. Measuring mathematical problem solving with the math dataset. *arXiv preprint arXiv:2103.03874*, 2021.
- Hu, E. J., Shen, Y., Wallis, P., Allen-Zhu, Z., Li, Y., Wang, S., Wang, L., Chen, W., et al. Lora: Low-rank adaptation of large language models. *ICLR*, 1(2):3, 2022.
- Huang, W., Liao, Y., Liu, J., He, R., Tan, H., Zhang, S., Li, H., Liu, S., and Qi, X. Mixture compressor for mixture-of-experts llms gains more. *arXiv preprint arXiv:2410.06270*, 2024.
- Jain, N., Han, K., Gu, A., Li, W.-D., Yan, F., Zhang, T., Wang, S., Solar-Lezama, A., Sen, K., and Stoica, I. Livecodebench: Holistic and contamination free evaluation of large language models for code. *arXiv preprint arXiv:2403.07974*, 2024.

- Jaiswal, A., Wang, J., Li, Y., Li, P., Chen, T., Wang, Z., Wang, C., Pang, R., and Du, X. Finding fantastic experts in moes: A unified study for expert dropping strategies and observations. *arXiv preprint arXiv:2504.05586*, 2025.
- Jiang, A. Q., Sablayrolles, A., Roux, A., Mensch, A., Savary, B., Bamford, C., Chaplot, D. S., Casas, D. d. l., Hanna, E. B., Bressand, F., et al. Mixtral of experts. *arXiv preprint arXiv:2401.04088*, 2024.
- Koishekenov, Y., Berard, A., and Nikoulina, V. Memory-efficient nllb-200: Language-specific expert pruning of a massively multilingual machine translation model. In *Proceedings of the 61st Annual Meeting of the Association for Computational Linguistics (Volume 1: Long Papers)*, pp. 3567–3585, 2023.
- Lasby, M., Lazarevich, I., Sinnadurai, N., Lie, S., Ioannou, Y., and Thangarasa, V. Reap the experts: Why pruning prevails for one-shot moe compression. *arXiv preprint arXiv:2510.13999*, 2025.
- Lee, J., Park, S., Mo, S., Ahn, S., and Shin, J. Layer-adaptive sparsity for the magnitude-based pruning. *arXiv preprint arXiv:2010.07611*, 2020.
- Lee, J., Hwang, S.-w., Qiao, A., Campos, D. F., Yao, Z., and He, Y. Stun: Structured-then-unstructured pruning for scalable moe pruning. In *Proceedings of the 63rd Annual Meeting of the Association for Computational Linguistics (Volume 1: Long Papers)*, pp. 13660–13676, 2025.
- Leviathan, Y., Kalman, M., and Matias, Y. Fast inference from transformers via speculative decoding. In *International Conference on Machine Learning*, pp. 19274–19286. PMLR, 2023.
- Li, P., Zhang, Z., Yadav, P., Sung, Y.-L., Cheng, Y., Bansal, M., and Chen, T. Merge, then compress: Demystify efficient smoe with hints from its routing policy. *arXiv preprint arXiv:2310.01334*, 2023.
- Li, W., Li, L., Gu, H., Huang, Y.-L., Lee, M. G., Sun, S., Xue, W., and Guo, Y. Moe-svd: Structured mixture-of-experts llms compression via singular value decomposition. In *Forty-second International Conference on Machine Learning*.
- Lin, B. Y., Deng, Y., Chandu, K., Brahman, F., Ravichander, A., Pyatkin, V., Dziri, N., Bras, R. L., and Choi, Y. Wild-bench: Benchmarking llms with challenging tasks from real users in the wild. *arXiv preprint arXiv:2406.04770*, 2024.
- Liu, A., Feng, B., Xue, B., Wang, B., Wu, B., Lu, C., Zhao, C., Deng, C., Zhang, C., Ruan, C., et al. Deepseek-v3 technical report. *arXiv preprint arXiv:2412.19437*, 2024a.
- Liu, E., Zhu, J., Lin, Z., Ning, X., Blaschko, M. B., Yan, S., Dai, G., Yang, H., and Wang, Y. Efficient expert pruning for sparse mixture-of-experts language models: Enhancing performance and reducing inference costs. *arXiv preprint arXiv:2407.00945*, 2024b.
- Liu, J., Xia, C. S., Wang, Y., and Zhang, L. Is your code generated by chatgpt really correct? rigorous evaluation of large language models for code generation. *Advances in Neural Information Processing Systems*, 36:21558–21572, 2023.
- Liu, J., Tang, P., Wang, W., Ren, Y., Hou, X., Heng, P.-A., Guo, M., and Li, C. A survey on inference optimization techniques for mixture of experts models. *arXiv preprint arXiv:2412.14219*, 2024c.
- Liu, S., Chen, T., Chen, X., Shen, L., Mocanu, D. C., Wang, Z., and Pechenizkiy, M. The unreasonable effectiveness of random pruning: Return of the most naive baseline for sparse training. *arXiv preprint arXiv:2202.02643*, 2022.
- Lu, H., Zhou, Y., Liu, S., Wang, Z., Mahoney, M. W., and Yang, Y. Alphapruning: Using heavy-tailed self regularization theory for improved layer-wise pruning of large language models. *Advances in neural information processing systems*, 37:9117–9152, 2024a.
- Lu, X., Liu, Q., Xu, Y., Zhou, A., Huang, S., Zhang, B., Yan, J., and Li, H. Not all experts are equal: Efficient expert pruning and skipping for mixture-of-experts large language models. *arXiv preprint arXiv:2402.14800*, 2024b.
- Meta, A. The llama 4 herd: The beginning of a new era of natively multimodal ai innovation. <https://ai.meta.com/blog/llama-4-multimodal-intelligence/>, checked on, 4(7):2025, 2025.
- Mihaylov, T., Clark, P., Khot, T., and Sabharwal, A. Can a suit of armor conduct electricity? a new dataset for open book question answering. *arXiv preprint arXiv:1809.02789*, 2018.
- Muennighoff, N., Soldaini, L., Groeneveld, D., Lo, K., Morrison, J., Min, S., Shi, W., Walsh, P., Tafjord, O., Lambert, N., et al. Olmoe: Open mixture-of-experts language models. *arXiv preprint arXiv:2409.02060*, 2024.
- Muzio, A., Sun, A., and He, C. Seer-moe: Sparse expert efficiency through regularization for mixture-of-experts. *arXiv preprint arXiv:2404.05089*, 2024.
- OpenAI. gpt-oss-120b & gpt-oss-20b model card, 2025. URL <https://arxiv.org/abs/2508.10925>.
- Sakaguchi, K., Bras, R. L., Bhagavatula, C., and Choi, Y. Winogrande: An adversarial winograd schema challenge at scale. *Communications of the ACM*, 64(9):99–106, 2021.

- Shazeer, N., Mirhoseini, A., Maziarz, K., Davis, A., Le, Q., Hinton, G., and Dean, J. Outrageously large neural networks: The sparsely-gated mixture-of-experts layer. *arXiv preprint arXiv:1701.06538*, 2017.
- Sun, M., Liu, Z., Bair, A., and Kolter, J. Z. A simple and effective pruning approach for large language models. *arXiv preprint arXiv:2306.11695*, 2023.
- Tang, S., Sieberling, O., Kurtic, E., Shen, Z., and Alishtarh, D. Darwinlm: Evolutionary structured pruning of large language models. *arXiv preprint arXiv:2502.07780*, 2025.
- Team, K., Bai, Y., Bao, Y., Chen, G., Chen, J., Chen, N., Chen, R., Chen, Y., Chen, Y., Chen, Y., et al. Kimi k2: Open agentic intelligence. *arXiv preprint arXiv:2507.20534*, 2025.
- Team, M. Evalscope: Evaluation framework for large models, 2024. URL <https://github.com/modelscope/evalscope>.
- Team, Q. Qwen1.5-moe: Matching 7b model performance with 1/3 activated parameters”, February 2024. URL <https://qwenlm.github.io/blog/qwen-moe/>.
- Vaswani, A., Shazeer, N., Parmar, N., Uszkoreit, J., Jones, L., Gomez, A. N., Kaiser, Ł., and Polosukhin, I. Attention is all you need. *Advances in neural information processing systems*, 30, 2017.
- Xie, Y., Zhang, Z., Zhou, D., Xie, C., Song, Z., Liu, X., Wang, Y., Lin, X., and Xu, A. Moe-pruner: Pruning mixture-of-experts large language model using the hints from its router. *arXiv preprint arXiv:2410.12013*, 2024.
- Yang, A., Li, A., Yang, B., Zhang, B., Hui, B., Zheng, B., Yu, B., Gao, C., Huang, C., Lv, C., et al. Qwen3 technical report. *arXiv preprint arXiv:2505.09388*, 2025.
- Yang, C., Sui, Y., Xiao, J., Huang, L., Gong, Y., Duan, Y., Jia, W., Yin, M., Cheng, Y., and Yuan, B. Moe-i<sup>2</sup>: Compressing mixture of experts models through inter-expert pruning and intra-expert low-rank decomposition. *arXiv preprint arXiv:2411.01016*, 2024.
- Yin, L., Wu, Y., Zhang, Z., Hsieh, C.-Y., Wang, Y., Jia, Y., Li, G., Jaiswal, A., Pechenizkiy, M., Liang, Y., et al. Outlier weighed layerwise sparsity (owl): A missing secret sauce for pruning llms to high sparsity. *arXiv preprint arXiv:2310.05175*, 2023.
- Zellers, R., Holtzman, A., Bisk, Y., Farhadi, A., and Choi, Y. Hellaswag: Can a machine really finish your sentence? *arXiv preprint arXiv:1905.07830*, 2019.
- Zeng, A., Lv, X., Zheng, Q., Hou, Z., Chen, B., Xie, C., Wang, C., Yin, D., Zeng, H., Zhang, J., et al. Glm-4.5: Agentic, reasoning, and coding (arc) foundation models. *arXiv preprint arXiv:2508.06471*, 2025.
- Zhang, Z., Liu, X., Cheng, H., Xu, C., and Gao, J. Diversifying the expert knowledge for task-agnostic pruning in sparse mixture-of-experts. In *Findings of the Association for Computational Linguistics: ACL 2025*, pp. 86–102, 2025.
- Zhou, Y., Zhao, Z., Cheng, D., Gui, J., Yang, Y., Wu, F., Cheng, Y., Fan, H., et al. Dropping experts, recombining neurons: Retraining-free pruning for sparse mixture-of-experts llms. *arXiv preprint arXiv:2509.10377*, 2025.

# Appendix

## A. Evolutionary Search Pseudocode

---

**Algorithm 1** Evolutionary Search for Non-uniform Layer-wise Sparsity Allocation
 

---

**Require:** Per-layer pruning orders  $\{\pi_\ell\}_{\ell=1}^L$ ; expert counts  $\{n_\ell\}$ ; fanouts  $\{k_\ell\}$ ; global budget  $B$ ; search dataset  $\mathcal{D}_{\text{search}} = \{(u^{(i)}, a^{(i)})\}_{i=1}^N$ ; fitness  $f(\mathbf{r}; \mathcal{D}_{\text{search}})$  (ESAP, Sec. 3.4); population size  $P$ ; elite size  $m$ ; generations  $T$ ; max transfer  $\Delta_{\text{max}}$ ; mutation cap  $\tau_{\text{max}}$ .

**Ensure:** Best allocation  $\mathbf{r}^*$ .

- 1: **Feasible set:**  $\mathcal{F} \triangleq \left\{ \mathbf{r} \in \mathbb{Z}^L \mid \sum_{\ell=1}^L r_\ell = B, 0 \leq r_\ell \leq n_\ell - k_\ell \forall \ell \right\}$ .
  - 2: **Init population**  $\mathcal{S}^{(0)} \subset \mathcal{F}$  of size  $P$  using (i) uniform, (ii) patterned seeds, and (iii) random feasible samples.
  - 3: **(Optional speedup)** Cache baseline (full-model) logits on  $\mathcal{D}_{\text{search}}$  under teacher forcing for reuse in  $f(\cdot; \mathcal{D}_{\text{search}})$ .
  - 4: Evaluate  $f(\mathbf{r}; \mathcal{D}_{\text{search}})$  for all  $\mathbf{r} \in \mathcal{S}^{(0)}$ .
  - 5:  $\mathbf{r}^* \leftarrow \arg \max_{\mathbf{r} \in \mathcal{S}^{(0)}} f(\mathbf{r}; \mathcal{D}_{\text{search}})$ .
  - 6: **for**  $t = 0, 1, \dots, T - 1$  **do**
  - 7:     **Selection:**  $\mathcal{S}_{\text{elite}}^{(t)} \leftarrow \text{TopM}(\mathcal{S}^{(t)}; f(\cdot; \mathcal{D}_{\text{search}}), m)$ .
  - 8:      $\mathcal{S}^{(t+1)} \leftarrow \mathcal{S}_{\text{elite}}^{(t)}$ .
  - 9:     **while**  $|\mathcal{S}^{(t+1)}| < P$  **do**
  - 10:         Sample parent  $\mathbf{r}$  uniformly from  $\mathcal{S}_{\text{elite}}^{(t)}$ .
  - 11:         Sample mutation count
 
$$\tau \leftarrow \min(U\{1, \dots, \tau_{\text{max}}\}, U\{1, \dots, \tau_{\text{max}}\}).$$
  - 12:          $\mathbf{r}' \leftarrow \mathbf{r}$ .
  - 13:         **for**  $i = 1, 2, \dots, \tau$  **do**
  - 14:             **repeat**
  - 15:                 Sample distinct layers  $a \neq b$  uniformly from  $\{1, \dots, L\}$ .
  - 16:                 Sample  $\Delta$  uniformly from  $\{1, 2, \dots, \Delta_{\text{max}}\}$ .
  - 17:                 Propose level-switch update:
 
$$\tilde{r}_\ell = \begin{cases} r'_\ell + \Delta, & \ell = a, \\ r'_\ell - \Delta, & \ell = b, \\ r'_\ell, & \text{otherwise.} \end{cases}$$
  - 18:                 **until**  $\tilde{\mathbf{r}} \in \mathcal{F}$
  - 19:                  $\mathbf{r}' \leftarrow \tilde{\mathbf{r}}$ .
  - 20:             **end for**
  - 21:              $\mathcal{S}^{(t+1)} \leftarrow \mathcal{S}^{(t+1)} \cup \{\mathbf{r}'\}$ .
  - 22:         **end while**
  - 23:         Evaluate  $f(\mathbf{r}; \mathcal{D}_{\text{search}})$  for all newly added  $\mathbf{r} \in \mathcal{S}^{(t+1)}$  if not yet evaluated.
  - 24:          $\mathbf{r}^* \leftarrow \arg \max_{\mathbf{r} \in \{\mathbf{r}^*\} \cup \mathcal{S}^{(t+1)}} f(\mathbf{r}; \mathcal{D}_{\text{search}})$ .
  - 25:     **end for**
  - 26: **return**  $\mathbf{r}^*$ .
- 

## B. Derivation of the Total-Variation Relation

In this appendix we derive the identity

$$\text{ESAP}(x) = 1 - \text{TV}(p(\cdot | x), q(\cdot | x)), \quad (18)$$

where  $p(\cdot | x)$  and  $q(\cdot | x)$  are categorical distributions over the vocabulary  $\mathcal{V}$ , and

$$\text{TV}(p, q) \triangleq \frac{1}{2} \sum_{v \in \mathcal{V}} |p(v | x) - q(v | x)|. \quad (19)$$

Table 6. MC and open-ended generation benchmark results for ERNIE-4.5-21B-A3B-PT under 25% global sparsity. Pruning is calibrated on C4. ESAP is the non-uniform allocation searched on `evol-codealpaca-v1` with the same pruning metric calibrated on `c4`.

Model	Sparsity	Method	Coding			Creative Writing WildBench	Math			MC MC Avg
			Eval+	LiveCode	Avg		GSM8K	MATH-500	Avg	
ERNIE	Full		0.867	0.247	0.557	0.479	0.829	0.780	0.804	0.721
		EAN	0.248	0.049	0.148	0.412	0.670	0.366	0.518	<b>0.685</b>
	25%	ESAP	<b>0.354</b>	<b>0.093</b>	<b>0.223</b>	<b>0.433</b>	<b>0.752</b>	<b>0.438</b>	<b>0.595</b>	0.669
		SEER	0.249	0.055	0.152	0.406	<b>0.738</b>	0.374	0.556	0.660
	Freq	UNI	0.269	<b>0.071</b>	0.170	0.355	0.636	0.304	0.470	0.655
		ESAP	<b>0.329</b>	0.049	<b>0.189</b>	<b>0.367</b>	<b>0.685</b>	<b>0.418</b>	<b>0.551</b>	<b>0.662</b>
	REAP	UNI	0.210	0.060	0.135	0.413	0.782	0.482	0.632	0.684
		ESAP	<b>0.401</b>	<b>0.132</b>	<b>0.267</b>	<b>0.435</b>	<b>0.817</b>	<b>0.616</b>	<b>0.716</b>	<b>0.692</b>

Recall the closed form of ESAP from (14):

$$ESAP(x) = \sum_{v \in \mathcal{V}} \min(p(v | x), q(v | x)). \tag{20}$$

We use the elementary identity valid for any  $a, b \geq 0$ :

$$\min(a, b) = \frac{1}{2}(a + b - |a - b|). \tag{21}$$

Applying (21) pointwise to each token  $v$  and summing gives

$$\begin{aligned} \sum_{v \in \mathcal{V}} \min(p(v | x), q(v | x)) &= \frac{1}{2} \sum_{v \in \mathcal{V}} (p(v | x) + q(v | x) - |p(v | x) - q(v | x)|) \\ &= \frac{1}{2} \left( \sum_{v \in \mathcal{V}} p(v | x) + \sum_{v \in \mathcal{V}} q(v | x) \right) - \frac{1}{2} \sum_{v \in \mathcal{V}} |p(v | x) - q(v | x)| \\ &= 1 - \frac{1}{2} \sum_{v \in \mathcal{V}} |p(v | x) - q(v | x)|, \end{aligned} \tag{22}$$

where we used  $\sum_v p(v | x) = \sum_v q(v | x) = 1$ . Recognizing the last term as the total-variation distance yields

$$ESAP(x) = 1 - TV(p(\cdot | x), q(\cdot | x)), \tag{23}$$

### C. Limitations

Our work has limitations: we currently assume a fixed within-layer pruning order and optimize only the across-layer allocation, leaving joint expert selection and allocation as an open problem, and the evolutionary search introduces additional compute overhead during compression. In future work, we aim to develop more efficient search strategies and to extend the framework to jointly optimize within-layer selection and layer-wise allocation under a fixed global budget.

### D. Results using C4 as calibration dataset

We also report the results that use C4 (Allen Institute for AI, 2024) which is a cleaned Common Crawl web-text corpus as calibration data in Table 6. All the hyperparameters are the same as mentioned in Section 4.1. Here we highlight two observations: (i) calibrating on C4 leads to a substantial drop on coding benchmarks compared to Table 1 (calibrated on `evol-codealpaca-v1`); and (ii) under the same C4 calibration setting, EVOESAP consistently improves performance.

### E. Visualization of searched sparsity distribution

Figure 3 visualizes the searched layer-wise density schedules (density = 1 - sparsity) produced by EvoESAP under four fixed within-layer pruning orders (EAN, SEER, Frequency, REAP) at two global sparsity levels. We show 25% sparsity in Figure 3a and 50% sparsity in Figure 3b, using the same experimental settings as Section 4.1. For clarity, we plot

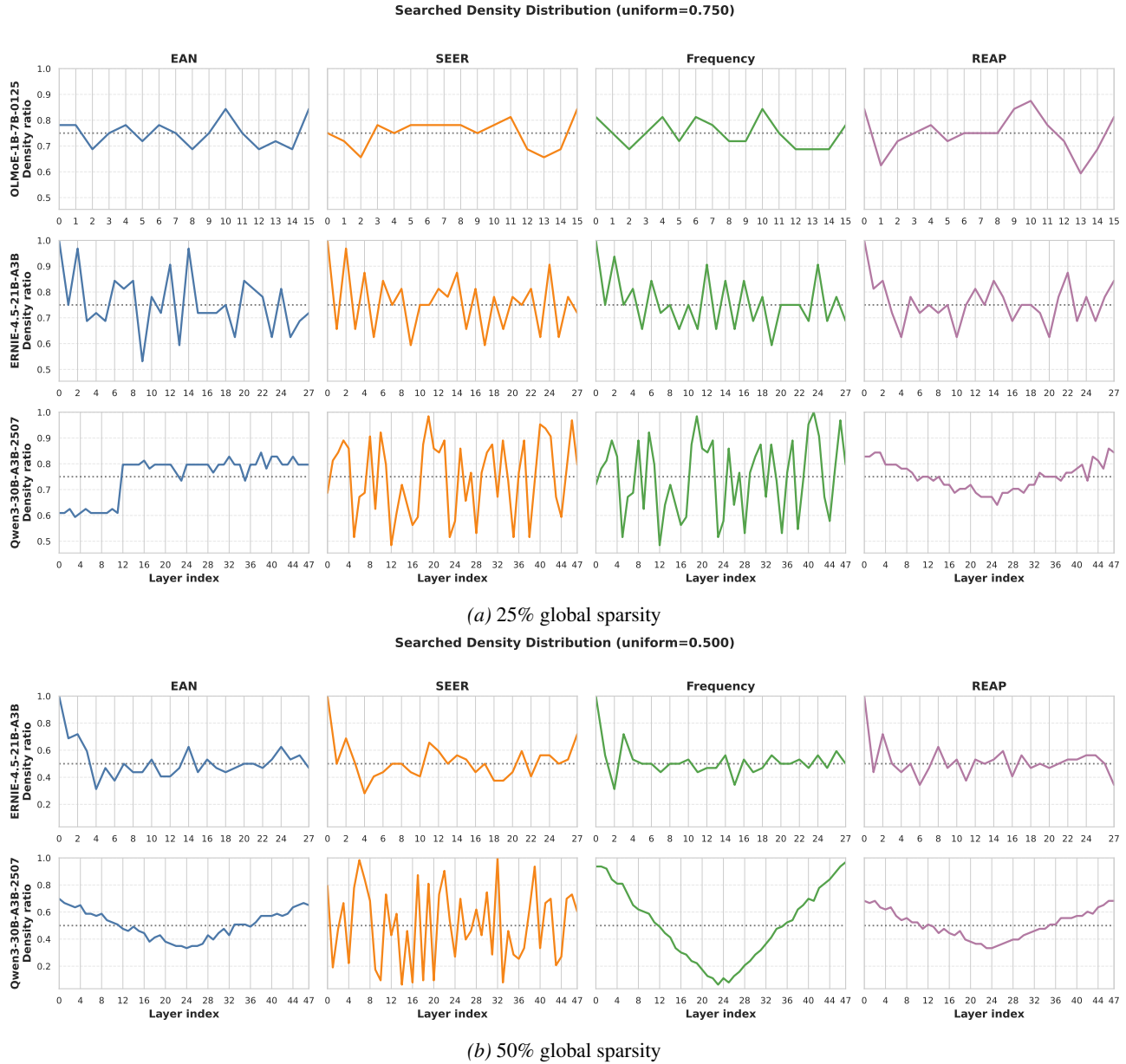


Figure 3. Layer-wise density distributions (density = 1 – sparsity) of the searched non-uniform allocations across different pruning metrics.

density rather than sparsity, since higher density directly reflects more retained capacity in each layer. Overall, the searched allocations are non-uniform, but their shapes are not consistent across pruning criteria or backbones, suggesting that there is no single universal allocation template. A particularly illustrative contrast appears at 50% sparsity: for ERNIE, the searched schedules across different pruning orders are relatively similar and fluctuate around the uniform, whereas for Qwen3 they vary substantially across criteria, with SEER inducing the largest deviations. These observations indicate that optimizing within-layer pruning orders alone is generally insufficient: the allocation that best preserves behavior can depend on both the model and the pruning criterion, making the discovery of effective non-uniform schedules non-trivial.

## F. Full evaluation results

Tables 7 to 9 extend the main results tables by reporting the per-benchmark scores, the main text reports only the aggregated averages.

Table 7. Full results on coding benchmarks. Eval+ is the average of HumanEval, HumanEval+, MBPP and MBPP+.

Model	Compression	Method		HumanEval	HumanEval+	MBPP	Coding		LiveCodeBench	Code Avg
							MBPP+	Eval+		
OLMoE-1B-7B-0125-Instruct	Baseline			0.354	0.323	0.373	0.312	0.341	0.033	0.187
	25%	EAN	UNIFORM	<b>0.366</b>	<b>0.341</b>	<b>0.360</b>	<b>0.307</b>	<b>0.343</b>	0.022	<b>0.183</b>
			SEARCHED	0.317	0.293	0.347	0.291	0.312	<b>0.027</b>	0.170
		SEER	UNIFORM	<b>0.360</b>	<b>0.341</b>	<b>0.349</b>	<b>0.307</b>	<b>0.339</b>	<b>0.027</b>	<b>0.183</b>
			SEARCHED	0.311	0.274	0.347	0.294	0.306	0.022	0.164
	Frequency	UNIFORM	<b>0.378</b>	<b>0.335</b>	0.349	0.302	0.341	<b>0.022</b>	<b>0.182</b>	
		SEARCHED	0.360	0.311	<b>0.376</b>	<b>0.320</b>	<b>0.342</b>	<b>0.022</b>	<b>0.182</b>	
	REAP	UNIFORM	0.341	0.311	0.331	0.272	0.314	0.005	0.160	
SEARCHED		<b>0.378</b>	<b>0.341</b>	<b>0.352</b>	<b>0.304</b>	<b>0.344</b>	<b>0.033</b>	<b>0.189</b>		
ERNIE-4.5-21B-A3B-PT	Baseline			0.909	0.878	0.915	0.765	0.867	0.247	0.557
	25%	EAN	UNIFORM	0.884	0.854	0.844	<b>0.728</b>	0.827	0.214	0.520
			SEARCHED	<b>0.902</b>	<b>0.866</b>	<b>0.847</b>	0.714	<b>0.832</b>	<b>0.225</b>	<b>0.528</b>
		SEER	UNIFORM	0.890	0.860	0.844	<b>0.725</b>	0.830	<b>0.214</b>	<b>0.522</b>
			SEARCHED	<b>0.909</b>	<b>0.866</b>	<b>0.852</b>	<b>0.725</b>	<b>0.838</b>	0.203	0.520
	Frequency	UNIFORM	<b>0.878</b>	<b>0.841</b>	<b>0.847</b>	<b>0.706</b>	<b>0.818</b>	0.181	0.499	
		SEARCHED	0.866	0.835	0.839	0.704	0.811	<b>0.236</b>	<b>0.524</b>	
	REAP	UNIFORM	0.872	0.841	0.860	0.717	0.823	<b>0.231</b>	<b>0.527</b>	
		SEARCHED	<b>0.896</b>	<b>0.848</b>	<b>0.865</b>	<b>0.722</b>	<b>0.833</b>	0.209	0.521	
	50%	EAN	UNIFORM	0.646	0.616	0.701	0.579	0.636	<b>0.148</b>	0.392
			SEARCHED	<b>0.677</b>	<b>0.646</b>	<b>0.714</b>	<b>0.601</b>	<b>0.659</b>	0.143	<b>0.401</b>
		SEER	UNIFORM	0.713	0.689	<b>0.759</b>	<b>0.630</b>	0.698	0.170	0.434
SEARCHED			<b>0.762</b>	<b>0.726</b>	0.730	0.619	<b>0.709</b>	<b>0.181</b>	<b>0.445</b>	
Frequency	UNIFORM	0.677	0.634	<b>0.704</b>	<b>0.574</b>	<b>0.647</b>	<b>0.143</b>	<b>0.395</b>		
	SEARCHED	<b>0.689</b>	<b>0.640</b>	0.690	0.569	<b>0.647</b>	0.126	0.387		
REAP	UNIFORM	0.768	0.726	<b>0.770</b>	0.656	0.730	<b>0.192</b>	0.461		
	SEARCHED	<b>0.774</b>	<b>0.738</b>	0.765	<b>0.669</b>	<b>0.737</b>	0.187	<b>0.462</b>		
Qwen3-30B-A3B-Instruct-2507	Baseline			0.939	0.902	0.892	0.751	0.871	0.368	0.619
	25%	EAN	UNIFORM	<b>0.945</b>	<b>0.896</b>	<b>0.886</b>	<b>0.757</b>	<b>0.871</b>	<b>0.363</b>	<b>0.617</b>
			SEARCHED	0.927	0.890	0.878	0.738	0.858	<b>0.363</b>	0.611
		SEER	UNIFORM	0.902	0.854	0.894	0.754	0.851	0.363	0.607
			SEARCHED	<b>0.915</b>	<b>0.872</b>	<b>0.897</b>	<b>0.759</b>	<b>0.861</b>	<b>0.385</b>	<b>0.623</b>
	Frequency	UNIFORM	<b>0.921</b>	<b>0.878</b>	<b>0.897</b>	0.751	<b>0.862</b>	0.357	0.609	
		SEARCHED	0.915	0.872	<b>0.897</b>	<b>0.757</b>	0.860	<b>0.396</b>	<b>0.628</b>	
	REAP	UNIFORM	<b>0.945</b>	<b>0.896</b>	<b>0.897</b>	<b>0.749</b>	<b>0.872</b>	<b>0.385</b>	<b>0.629</b>	
		SEARCHED	0.896	0.866	0.862	0.714	0.835	0.324	0.580	
	50%	EAN	UNIFORM	<b>0.915</b>	<b>0.878</b>	<b>0.865</b>	<b>0.725</b>	<b>0.846</b>	0.341	<b>0.594</b>
			SEARCHED	<b>0.915</b>	0.866	0.860	0.714	0.839	<b>0.346</b>	0.593
		SEER	UNIFORM	0.774	0.713	0.720	0.593	0.700	0.247	0.473
SEARCHED			<b>0.872</b>	<b>0.817</b>	<b>0.757</b>	<b>0.622</b>	<b>0.767</b>	<b>0.264</b>	<b>0.516</b>	
Frequency	UNIFORM	0.787	0.738	0.701	0.574	0.700	0.225	0.462		
	SEARCHED	<b>0.872</b>	<b>0.817</b>	<b>0.788</b>	<b>0.648</b>	<b>0.781</b>	<b>0.275</b>	<b>0.528</b>		
REAP	UNIFORM	0.902	0.854	0.857	0.698	0.828	<b>0.341</b>	0.585		
	SEARCHED	<b>0.939</b>	<b>0.902</b>	<b>0.868</b>	<b>0.709</b>	<b>0.855</b>	0.335	<b>0.595</b>		

Table 8. Full results on WildBench and math benchmarks.

Model	Compression	Method		WildBench + Math			
				WildBench	GSM8K	MATH-500	Math Avg
OLMoE-1B-7B-0125-Instruct	Baseline			0.444	0.682	0.222	0.452
	25%	EAN	UNIFORM	<b>0.269</b>	<b>0.585</b>	0.190	0.387
			SEARCHED	0.258	0.576	<b>0.232</b>	<b>0.404</b>
		SEER	UNIFORM	0.253	0.577	0.204	0.390
			SEARCHED	<b>0.254</b>	<b>0.601</b>	<b>0.248</b>	<b>0.424</b>
	Frequency	UNIFORM	<b>0.265</b>	0.591	<b>0.220</b>	<b>0.406</b>	
SEARCHED		0.244	<b>0.596</b>	0.208	0.402		
REAP	UNIFORM	<b>0.292</b>	0.596	0.200	0.398		
		SEARCHED	0.279	<b>0.636</b>	<b>0.216</b>	<b>0.426</b>	
ERNIE-4.5-21B-A3B-PT	Baseline			0.479	0.829	0.780	0.804
	25%	EAN	UNIFORM	<b>0.377</b>	0.815	0.748	0.781
			SEARCHED	0.333	<b>0.823</b>	<b>0.772</b>	<b>0.798</b>
		SEER	UNIFORM	<b>0.301</b>	<b>0.804</b>	<b>0.736</b>	<b>0.770</b>
			SEARCHED	0.291	<b>0.804</b>	0.728	0.766
	Frequency	UNIFORM	0.314	0.810	0.692	0.751	
		SEARCHED	<b>0.316</b>	<b>0.815</b>	<b>0.716</b>	<b>0.765</b>	
	REAP	UNIFORM	0.354	<b>0.821</b>	0.730	0.776	
		SEARCHED	<b>0.376</b>	0.814	<b>0.752</b>	<b>0.783</b>	
	50%	EAN	UNIFORM	0.156	<b>0.748</b>	0.542	0.645
			SEARCHED	<b>0.186</b>	0.744	<b>0.558</b>	<b>0.651</b>
		SEER	UNIFORM	0.130	0.555	0.418	0.487
SEARCHED			<b>0.151</b>	<b>0.640</b>	<b>0.508</b>	<b>0.574</b>	
Frequency	UNIFORM	0.130	0.522	0.272	0.397		
	SEARCHED	<b>0.151</b>	<b>0.631</b>	<b>0.468</b>	<b>0.549</b>		
REAP	UNIFORM	<b>0.215</b>	0.695	<b>0.598</b>	0.646		
	SEARCHED	0.205	<b>0.718</b>	0.578	<b>0.648</b>		
Qwen3-30B-A3B-Instruct-2507	Baseline			0.644	0.923	0.802	0.862
	25%	EAN	UNIFORM	<b>0.517</b>	<b>0.902</b>	0.748	0.825
			SEARCHED	0.439	0.901	<b>0.752</b>	<b>0.826</b>
		SEER	UNIFORM	0.449	0.891	0.636	0.763
			SEARCHED	<b>0.482</b>	<b>0.897</b>	<b>0.716</b>	<b>0.806</b>
	Frequency	UNIFORM	0.446	0.891	0.658	0.774	
		SEARCHED	<b>0.463</b>	<b>0.907</b>	<b>0.734</b>	<b>0.821</b>	
	REAP	UNIFORM	<b>0.565</b>	<b>0.910</b>	<b>0.784</b>	<b>0.847</b>	
		SEARCHED	0.533	0.886	0.778	0.832	
	50%	EAN	UNIFORM	0.231	0.833	0.456	0.645
			SEARCHED	<b>0.243</b>	<b>0.846</b>	<b>0.494</b>	<b>0.670</b>
		SEER	UNIFORM	0.112	<b>0.605</b>	0.144	<b>0.374</b>
SEARCHED			<b>0.142</b>	0.550	<b>0.220</b>	<b>0.385</b>	
Frequency	UNIFORM	0.110	0.592	0.128	0.360		
	SEARCHED	<b>0.182</b>	<b>0.697</b>	<b>0.214</b>	<b>0.455</b>		
REAP	UNIFORM	<b>0.299</b>	<b>0.872</b>	<b>0.798</b>	<b>0.835</b>		
	SEARCHED	0.267	0.867	0.792	0.829		

EvoESAP: Non-Uniform Expert Pruning for Sparse MoE

Table 9. Full results on multiple-choice benchmarks.

Model	Compression	Method	Multiple Choice									
			MMLU	ARC-C	ARC-E	HellaSwag	WinoGrande	BoolQ	OpenBookQA	RTE	MC Avg	
OLMoE-1B-7B-0125-Instruct	Baseline		0.534	0.490	0.758	0.808	0.684	0.766	0.470	0.711	0.653	
	25%	EAN	UNIFORM SEARCHED	0.452	<b>0.358</b>	0.558	<b>0.630</b>	<b>0.602</b>	<b>0.727</b>	<b>0.336</b>	<b>0.747</b>	<b>0.551</b>
				<b>0.454</b>	0.349	<b>0.573</b>	0.628	0.597	0.716	0.326	0.700	0.543
		SEER	UNIFORM SEARCHED	<b>0.457</b>	<b>0.352</b>	0.566	0.620	0.599	<b>0.723</b>	<b>0.340</b>	<b>0.708</b>	<b>0.545</b>
				0.447	0.338	<b>0.573</b>	<b>0.621</b>	<b>0.601</b>	0.715	0.330	0.690	0.539
	Frequency	UNIFORM SEARCHED	0.450	<b>0.351</b>	<b>0.572</b>	<b>0.621</b>	<b>0.605</b>	<b>0.727</b>	<b>0.334</b>	<b>0.718</b>	<b>0.547</b>	
			<b>0.455</b>	0.347	0.570	0.612	0.595	0.719	0.318	0.693	0.539	
	REAP	UNIFORM SEARCHED	<b>0.475</b>	0.418	0.625	0.680	0.637	<b>0.729</b>	0.362	<b>0.704</b>	0.579	
			0.474	<b>0.427</b>	<b>0.641</b>	<b>0.685</b>	<b>0.639</b>	0.712	<b>0.386</b>	0.682	<b>0.581</b>	
ERNIE-4.5-21B-A3B-PT	Baseline		0.739	0.564	0.782	0.814	0.717	0.872	0.462	0.816	0.721	
	25%	EAN	UNIFORM SEARCHED	0.625	0.496	0.710	0.719	0.705	0.862	<b>0.408</b>	<b>0.827</b>	0.669
				<b>0.646</b>	<b>0.509</b>	<b>0.725</b>	<b>0.731</b>	<b>0.708</b>	<b>0.864</b>	0.404	0.809	<b>0.675</b>
		SEER	UNIFORM SEARCHED	0.628	<b>0.466</b>	0.687	0.655	0.655	<b>0.856</b>	0.342	<b>0.780</b>	0.634
				<b>0.638</b>	<b>0.466</b>	<b>0.693</b>	<b>0.663</b>	<b>0.665</b>	0.843	<b>0.368</b>	0.773	<b>0.638</b>
		Frequency	UNIFORM SEARCHED	0.608	0.460	0.682	0.669	<b>0.671</b>	0.846	0.364	0.791	0.636
				<b>0.632</b>	<b>0.480</b>	<b>0.700</b>	<b>0.676</b>	0.662	<b>0.850</b>	<b>0.382</b>	<b>0.794</b>	<b>0.647</b>
		REAP	UNIFORM SEARCHED	<b>0.643</b>	<b>0.521</b>	0.756	0.718	0.692	<b>0.855</b>	0.404	0.747	0.667
				0.638	0.510	<b>0.764</b>	<b>0.719</b>	<b>0.698</b>	0.852	<b>0.408</b>	<b>0.787</b>	<b>0.672</b>
	50%	EAN	UNIFORM SEARCHED	<b>0.510</b>	0.417	<b>0.623</b>	<b>0.575</b>	0.631	0.836	<b>0.328</b>	<b>0.762</b>	<b>0.585</b>
				0.508	<b>0.424</b>	0.622	0.568	<b>0.642</b>	<b>0.839</b>	0.318	0.736	0.582
		SEER	UNIFORM SEARCHED	0.494	<b>0.396</b>	0.579	<b>0.505</b>	<b>0.606</b>	<b>0.811</b>	<b>0.300</b>	<b>0.718</b>	<b>0.551</b>
			<b>0.503</b>	0.394	<b>0.595</b>	0.484	0.591	0.800	0.298	0.708	0.547	
	Frequency	UNIFORM SEARCHED	<b>0.519</b>	<b>0.406</b>	<b>0.592</b>	<b>0.521</b>	<b>0.597</b>	<b>0.829</b>	0.292	<b>0.765</b>	<b>0.565</b>	
			0.508	0.397	0.586	0.497	0.575	0.821	<b>0.316</b>	0.755	0.557	
	REAP	UNIFORM SEARCHED	0.502	0.407	0.622	<b>0.556</b>	0.625	<b>0.814</b>	<b>0.344</b>	<b>0.733</b>	<b>0.575</b>	
			<b>0.508</b>	<b>0.410</b>	<b>0.637</b>	0.554	<b>0.627</b>	0.804	0.334	0.726	<b>0.575</b>	
Qwen3-30B-A3B-Instruct-2507	Baseline		0.802	0.625	0.838	0.797	0.736	0.887	0.446	0.769	0.737	
	25%	EAN	UNIFORM SEARCHED	<b>0.635</b>	0.451	0.636	<b>0.655</b>	0.676	<b>0.862</b>	0.338	<b>0.769</b>	0.628
				0.598	<b>0.491</b>	<b>0.674</b>	0.645	<b>0.692</b>	0.857	<b>0.354</b>	0.758	<b>0.634</b>
		SEER	UNIFORM SEARCHED	<b>0.533</b>	0.372	0.457	0.609	0.597	0.849	0.306	<b>0.765</b>	0.561
				0.495	<b>0.400</b>	<b>0.509</b>	<b>0.637</b>	<b>0.629</b>	<b>0.859</b>	<b>0.344</b>	0.744	<b>0.577</b>
		Frequency	UNIFORM SEARCHED	<b>0.527</b>	0.370	0.457	0.611	0.582	0.846	0.312	<b>0.762</b>	0.558
				0.494	<b>0.404</b>	<b>0.500</b>	<b>0.630</b>	<b>0.616</b>	<b>0.852</b>	<b>0.340</b>	0.740	<b>0.572</b>
		REAP	UNIFORM SEARCHED	<b>0.734</b>	<b>0.584</b>	<b>0.803</b>	<b>0.737</b>	<b>0.733</b>	<b>0.883</b>	<b>0.404</b>	0.773	<b>0.706</b>
				0.662	0.514	0.758	0.670	0.702	0.866	0.366	<b>0.780</b>	0.665
	50%	EAN	UNIFORM SEARCHED	0.464	<b>0.341</b>	<b>0.475</b>	0.483	<b>0.594</b>	0.791	0.298	0.679	0.516
				<b>0.465</b>	0.322	0.473	<b>0.489</b>	0.590	<b>0.803</b>	<b>0.310</b>	<b>0.690</b>	<b>0.518</b>
		SEER	UNIFORM SEARCHED	<b>0.421</b>	<b>0.284</b>	0.352	<b>0.448</b>	0.524	<b>0.702</b>	0.282	<b>0.625</b>	<b>0.455</b>
			0.412	0.274	<b>0.357</b>	0.438	<b>0.538</b>	0.695	<b>0.284</b>	0.567	0.446	
	Frequency	UNIFORM SEARCHED	0.421	0.294	0.346	0.447	0.515	0.695	0.284	0.596	0.450	
			<b>0.431</b>	<b>0.309</b>	<b>0.498</b>	<b>0.500</b>	<b>0.593</b>	<b>0.754</b>	<b>0.306</b>	<b>0.686</b>	<b>0.510</b>	
	REAP	UNIFORM SEARCHED	<b>0.591</b>	<b>0.459</b>	<b>0.652</b>	<b>0.543</b>	<b>0.668</b>	<b>0.813</b>	0.328	0.718	<b>0.596</b>	
			0.576	0.437	0.638	0.518	0.629	0.805	<b>0.332</b>	<b>0.747</b>	0.585	